

# Polycyclic Aromatic Carbon: A Key Fraction Determining the Light Absorption Properties of Methanol-Soluble Brown Carbon of Open Biomass Burning Aerosols

Yue Sun, Jiao Tang, Yangzhi Mo, Xiaofei Geng, Guangcai Zhong,\* Xin Yi, Caiqing Yan, Jun Li, and Gan Zhang\*



Cite This: *Environ. Sci. Technol.* 2021, 55, 15724–15733



Read Online

ACCESS |



Metrics & More



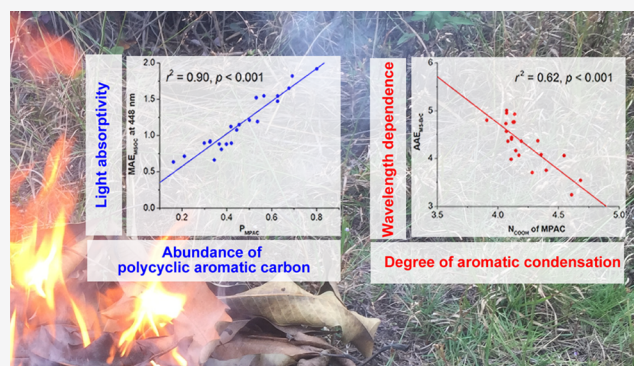
Article Recommendations



Supporting Information

**ABSTRACT:** The composition and radiative forcing of light-absorbing brown carbon (BrC) aerosol remain poorly understood. Polycyclic aromatics (PAs) are BrC chromophores with fused benzene rings. Understanding the occurrence and significance of PAs in BrC is challenging due to a lack of standards for many PAs. In this study, we quantified polycyclic aromatic carbon (PAC), defined as the carbon of fused benzene rings, based on molecular markers (benzene polycarboxylic acids, BPCAs). Open biomass burning aerosols (OBBAs) of 22 rainforest plants were successively extracted with water and methanol for the analysis of water- and methanol-soluble PAC (WPAC and MPAC, respectively). PAC is an important fraction of water- and methanol-soluble organic carbon (WSOC and MSOC, respectively). WPAC/WSOC ranged from 0.03 to 0.18, and MPAC/MSOC was even higher (range: 0.16–0.80). The priority polycyclic aromatic hydrocarbons contributed less than 1% of MPAC. The mass absorption efficiency (MAE) of MSOC showed a strong linear correlation with MPAC/MSOC ( $r = 0.60–0.95$ ,  $p < 0.01$ ). The absorption Ångström exponent (AAE) of methanol-soluble BrC showed a strong linear correlation with the degree of aromatic condensation of MPAC, which was described by the average number of carboxylic groups of BPCA ( $r = -0.79$ ,  $p < 0.01$ ). This result suggested that PAC was a key fraction determining the light absorption properties (i.e., light absorptivity and wavelength dependence) of methanol-soluble BrC in OBBAs.

**KEYWORDS:** brown carbon, polycyclic aromatics, biomass burning, benzene polycarboxylic acid, polycyclic aromatic hydrocarbons, mass absorption efficiencies, absorption Ångström exponents



## INTRODUCTION

Carbonaceous aerosols affect the Earth's radiative balance by scattering and absorbing sunlight.<sup>1,2</sup> Atmospheric carbonaceous aerosols, including black carbon (BC) and organic carbon (OC) aerosols, are attributed to various anthropogenic or natural sources.<sup>3,4</sup> BC is a well-known light absorber. BC absorbs solar radiation over a broad range from ultraviolet (UV) to infrared.<sup>3</sup> BC is identified as the second most potent global warming agent after carbon dioxide.<sup>4</sup> The OC fraction also absorbs sunlight, with absorption sharply increasing from the visible to the UV range.<sup>3</sup> This light-absorbing OC is termed brown carbon (BrC). Unlike BC, BrC consists of a wide range of compounds, which remain poorly characterized.<sup>5–13</sup> This lack of characterization is an obstacle for studies of the radiative forcing of BrC.

Polycyclic aromatics (PAs) are chemicals with fused benzene rings, which are BrC chromophores due to their polyconjugated  $\pi$  bonds. PAs in ambient aerosols are produced by incomplete combustion of organic matter, such as fossil fuel

and biomass.<sup>14</sup> Selected PAs, including priority polycyclic aromatic hydrocarbons (PAHs) and their derivatives, have been widely studied due to their occurrence in atmospheric aerosols.<sup>15–19</sup> Light absorption by these PAHs and their derivatives can be quantitatively understood based on standards, but they were shown to contribute no more than a few percent of the light absorption of BrC in biomass burning aerosols.<sup>20</sup> It is a major challenge to determine the occurrence and light absorption characteristics of the remaining PA constituents, the molecular structures of which are yet to be identified or for which standards are not commercially available.

**Received:** September 24, 2021

**Revised:** November 1, 2021

**Accepted:** November 9, 2021

**Published:** November 22, 2021



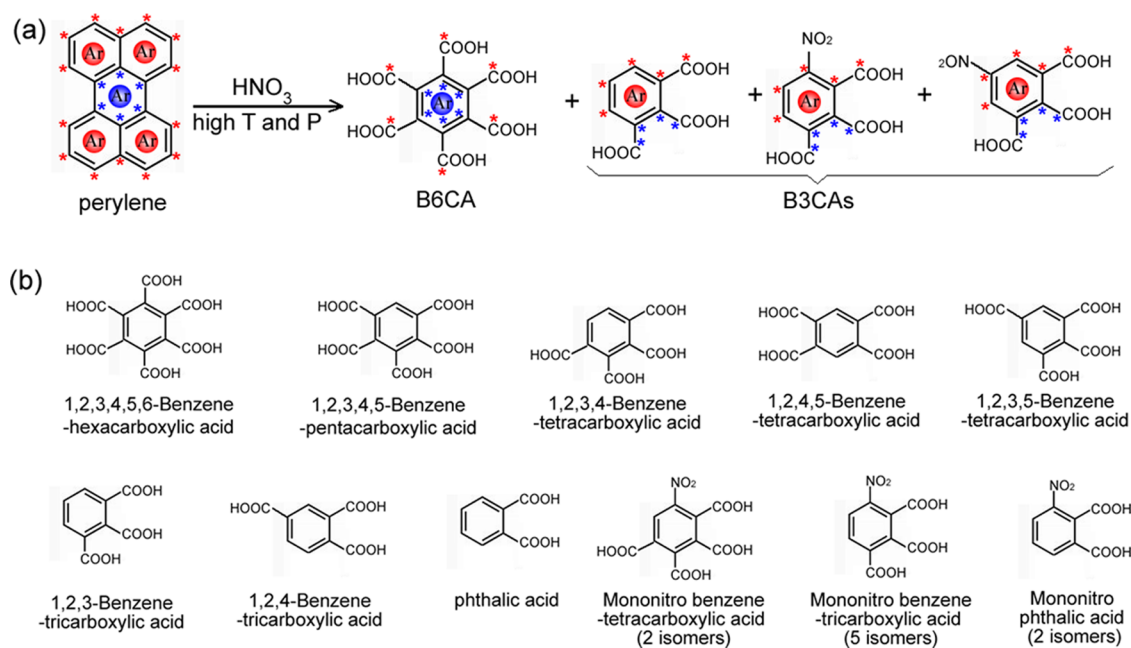


**Figure 1.** Principles of the BPCA method. (a) An example of conversion of fused benzene rings into BPCAs during nitric acid oxidation under conditions of high temperature and pressure. The blue/red stars and circles are used to track the C atoms and aromatic rings, respectively. (b) Possible BPCA products generated by nitric acid oxidation of PAC in aerosols.<sup>32</sup>

Here, we propose a method for quantifying polycyclic aromatic carbon (PAC), which is defined as the carbon of fused benzene rings, based on molecular markers (i.e., benzene polycarboxylic acids, BPCAs). In the BPCA method, fused benzene rings are converted into a single aromatic ring substituted with 2–6 carboxylic groups and 0–2 nitro group(s), i.e., BPCAs (Figure 1).<sup>21,22</sup> PAC can be calculated from the carbon content of BPCA products (BPCA-C) multiplied by a conversion factor.<sup>22</sup> The BPCA method has been widely used to analyze dissolved black carbon (DBC) in aquatic environments,<sup>23–28</sup> as well as BC in soils, sediments, and suspended particles in aquatic environments.<sup>21,29,30</sup> In these studies, DBC and BC were actually water-soluble PAC and insoluble PAC (in water and organic solvents) with highly condensed aromatic structures, respectively. The BPCA method was used in a recent study to analyze the DBC of ambient aerosols, but the discussion did not refer to BrC or light-absorbing aerosols.<sup>31</sup>

In the present study, 22 types of open biomass burning aerosol (OBBA) were successively extracted with water and methanol for the analysis of PAC and light absorption of BrC. Biomass burning has been identified as a significant contributor to BrC, and open biomass burning is an important type of biomass burning activity.<sup>33</sup> Solvent extraction is a common approach for research on BrC as it separates a large fraction of BrC from BC.<sup>3,9,34</sup> The light absorption characteristics of water- and methanol-soluble BrC (WS-BrC and MS-BrC, respectively) were measured as those of the water and methanol extracts, respectively, in the present study. Bulk water- and methanol-soluble PAC (WPAC and MPAC, respectively) were quantified with the BPCA method. The occurrence of WPAC and MPAC and the significance of PAC in the BrC of OBBA will be discussed.

## MATERIALS AND METHODS

**Collection of Biomass Burning Aerosols.** OBBA was produced by simulated open burning of 22 rainforest plants typical of Southeast Asia, including herbs, shrubs, and evergreen and deciduous trees (Table S1). Aerosol particles were collected on  $8 \times 10$  in. quartz filters. The collection of these filter samples was described previously<sup>12,35,36</sup> and in Section S1. Briefly, the dried plants (approximately  $20 \times 3 \times 2$  cm<sup>3</sup>) were ignited and combusted in a stainless steel bowl 40 cm in diameter. All plants were burned three times. Approximately 1–2 kg of fuel was consumed in each burn. The resultant smoke was introduced into the sampling system, and the particles were collected with particulate matter samplers after dilution. Collection of smoke particles was carried out beginning from when the fuels were ignited and ending when the  $\text{CO}_2$  concentration decreased to the atmospheric level. The quartz filters for smoke particle sampling were baked at 450 °C for 5 h before sampling. The filter samples were stored at –20 °C prior to analysis.

**Extraction and Nitric Acid Oxidation of PAC.** A punch (50 mm in diameter) of filter samples was successively extracted ultrasonically with ultrapure water and methanol. The extraction with each solvent was repeated three times using 20 mL of the solvent for 20 min each time. The water extracts were combined and filtered through a syringe filter (0.22  $\mu\text{m}$  pore size, poly(tetrafluoroethylene) (PTFE); ANPEL Laboratory Technologies, Shanghai, China), as were the methanol extracts. The methanol extract was evaporated to 1 mL using a rotary evaporator and further dried in 10 mL ampoules ( $A_1$ ) under a gentle stream of high-purity nitrogen gas (99.999%). The dried extract in  $A_1$  was analyzed for MPAC later.

WPAC in marine and fresh water samples is often isolated by reverse-phase solid-phase extraction (SPE),<sup>23,25,27</sup> so reverse-phase SPE was also used to isolate WPAC from the water extracts of aerosols in this study. The water extract of

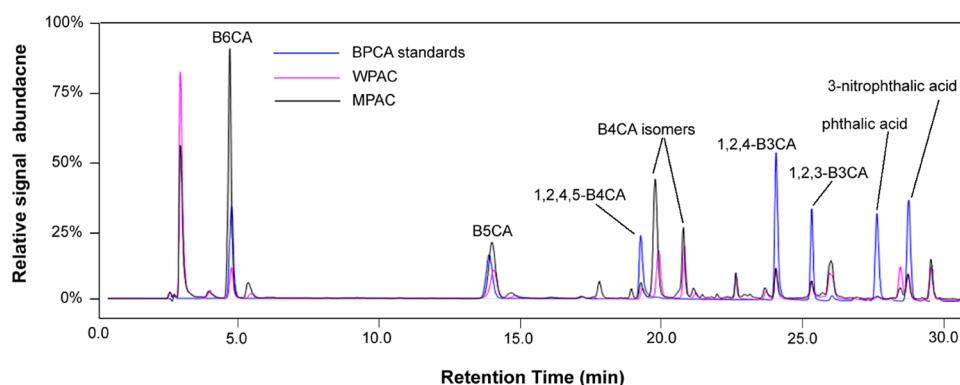


**Figure 2.** Representative HPLC-PAD chromatograms of BPCAs produced by nitric acid oxidation of WPAC and MPAC of OBBA.

OBBA was adjusted to pH 2 and passed through an Oasis HLB SPE cartridge (200 mg, 6 mL; Waters Oasis, Columbus, OH), which is widely used to isolate humic-like substances (HULIS) from water extracts of aerosols.<sup>9,36</sup> The breakthrough of the WPAC was checked using tandem cartridges and was less than 1%. Before absorption, the cartridge was conditioned with 6 mL of methanol and equilibrated with 6 mL of hydrochloric acid (pH 2). After absorption, the cartridge was eluted with 10 mL of methanol. The eluate was dried in a 10 mL ampoule (A<sub>2</sub>) under a stream of nitrogen gas and later analyzed for WPAC.

PACs in the ampoules, i.e., MPAC in A<sub>1</sub> and WPAC in A<sub>2</sub>, were converted to BPCAs under nitric acid oxidation.<sup>32</sup> The ampoules were sealed and placed into a 100 mL Teflon-lined stainless steel reaction vessel after the addition of 2 mL of 65% HNO<sub>3</sub> (Sigma-Aldrich, St. Louis, MO). The reaction vessel was tightly closed and then heated in an oven at 180 °C for 8 h. To prevent explosion of the ampoules caused by heating, 100  $\mu$ L of water was added to the reaction vessels before heating to balance the vapor pressure inside and outside the ampoules. When the reaction vessel had cooled completely, the ampoules were removed from the reaction vessel and opened in a fume hood. The samples were transferred from the ampoules to 4 mL vials, dried under a stream of nitrogen gas at 50 °C, and redissolved in 1 mL of ultrapure water. They were filtered with syringe filters (0.22  $\mu$ m pore size, PTFE; ANPEL Laboratory Technologies) prior to measurement of BPCAs by high-performance liquid chromatography (HPLC, LC-20AT; Shimadzu, Kyoto, Japan) equipped with a photodiode array detector (PAD, SPD-M20A; Shimadzu).

**Measurement of BPCAs.** BPCAs can be measured directly by HPLC-PAD and HPLC coupled to mass spectrometry (HPLC-MS) or by gas chromatography coupled to a flame ionization detector or mass spectrometry (GC-FID or GC-MS, respectively) after derivatization.<sup>21–23,37</sup> The reproducibility of the LC method is better than that of the GC method in most cases.<sup>37,38</sup> The use of MS for detection is beneficial for peak identification. Previously, we identified 17 BPCAs generated by nitric acid oxidation of water- and dichloromethane-soluble PAC of an urban aerosol sample with GC-MS (Figure 1b).<sup>32</sup> Improved reproducibility was also obtained by correcting the BPCA concentrations with the recoveries of deuterated PAH added to the samples. However, detection of BPCAs was carried out by HPLC-PAD in the present study because this method also allowed satisfactory peak identification (Figure 2) and was convenient and cost-effective.

The HPLC-PAD method was similar to that described previously.<sup>39</sup> An Agilent Infinity Lab Poroshell 120 SB-C18 (100 mm  $\times$  4.6 mm, 2.7  $\mu$ m) column (Agilent Technologies, Santa Clara, CA) was used for BPCA separation. HPLC-grade acetonitrile (Sigma-Aldrich) was used as mobile phase B. Mobile phase A was prepared by mixing 20 mL of phosphoric acid (85%; Sigma-Aldrich) with 980 mL of ultrapure water and filtered through a mixed cellulose ester filter (0.22  $\mu$ m pore size; ANPEL Laboratory Technologies) before use. The mixing gradients of mobile phases A and B are shown in Table S2. The total flow rate of the mobile phases was 0.4 mL/min, the oven temperature was 30 °C, and the injection volume was 10  $\mu$ L. Peak identification of BPCAs was based on retention time and absorption spectra (190–400 nm). The signal abundance of BPCA peaks at a wavelength of 240 nm was used for subsequent quantification.

Nine BPCAs, i.e., 1,2,3,4,5,6-benzenhexacarboxylic acid (B6CA), 1,2,3,4,5-benzenepentacarboxylic acid (B5CA), 1,2,4,5-benzenetetracarboxylic acid and its two isomers (i.e., 1,2,3,5-/1,2,3,4-benzenetetracarboxylic acid, B4CAs), 1,2,3-benzenetricarboxylic acid, 1,2,4-benzenetricarboxylic acid (B3CAs), phthalic acid, and 3-nitrophthalic acid (B2CAs), were measured. BPCAs were quantified using external calibration curves prepared with standard solutions (3.2, 4.8, 6.4, 8, 16, 32, 48, 64, 80 ng/ $\mu$ L), except for 1,2,3,5-B4CA and 1,2,3,4-B4CA, as standards for these two BPCAs are not commercially available; these BPCAs were quantified using the calibration curve of their isomer (i.e., 1,2,4,5-B4CA) as described in previous reports.<sup>23,38,39</sup> Mononitro-B4CAs and mononitro-B3CAs (Figure 1b) were not measured due to a lack of standards. Peaks not identified on the HPLC-PAD chromatogram likely corresponded to these compounds. The nine BPCAs quantified seemed to represent a large proportion of the total BPCAs based on chromatographic signal abundance (Figure 2).

Some BPCAs, including phthalic acid, mononitro-phthalic acids, 1,2,3-B3CAs, and 1,2,4-B3CAs, occur in aerosols directly released by various sources or exist in secondary organic aerosols,<sup>40–42</sup> but these native BPCAs did not seem to interfere with the measurement of the BPCAs produced by nitric acid oxidation of PAC, due to their low levels. The native BPCAs in OBBA should be extracted together with WPAC by ultrapure water due to their high polarity, so the interference of native BPCAs in the quantification of BPCAs produced by nitric acid oxidation of WPAC deserves attention. Phthalic acid is generally the most abundant native BPCA in organic aerosols,<sup>40–42</sup> whereas its abundance in BPCAs obtained after

nitric acid oxidation of WPAC was very low (Figure 2). This suggested that native BPCAs should be much less abundant than the BPCAs produced by nitric acid oxidation of WPAC.

**Calculation of PAC.** The conversion from the amount of BPCA to the amount of PAC was performed using model chemicals. The BPCA method was developed to analyze highly insoluble condensed PAC (i.e., BC) in soils by Glaser et al.<sup>21</sup> and the WPAC in seawater by Dittmar.<sup>23</sup> Glaser et al.<sup>21</sup> derived a conversion factor of 2.27 from BPCA-C to BC using activated charcoals as model chemicals. Indeed, the aromaticity and degree of aromatic condensation of charcoal were later found to vary according to the conditions (e.g., temperature) under which it formed. The carbon of activated charcoals may not be solely PAC, so PAC may be underestimated by multiplying BPCA-C with a conversion factor of 2.27. Dittmar<sup>23</sup> derived an equation to calculate the WPAC in seawater based on their typical molecular structures identified by ultrahigh-resolution MS. This calculation is restricted to these typical molecular structures, and is not suitable for other molecular structures of PAC.

There should be a conversion factor that is suitable for a wide range of molecular structures of PAC. Ziolkowski et al.<sup>22</sup> derived a conversion factor of  $4 \pm 1$  from BPCA-C to PAC based on pure PAC or chemicals highly enriched with PAC (i.e., nine PAHs, fullerenes, carbon nanotubes, hexane soot, and carbon lamp black). These model chemicals cover a wide range of molecular structures from small to large condensed aromatic systems. BPCA methods carried out by different research groups differ slightly in the time, temperature, and reaction vessels used for nitric acid oxidation,<sup>21–23,28</sup> which may lead to some variations in conversion factors. This deserves attention when calculating PAC with a conversion factor obtained from the literature. In our previous study, we determined a conversion factor of 5.7 based on four PAHs.<sup>32</sup> The difference in conversion factors between our previous study and that of Ziolkowski et al.<sup>22</sup> may be due to the different reaction vessels used and is likely to be systematic. For example, BPCA-C yields of two PAHs (i.e., phenanthrene and perylene) after nitric acid oxidation were determined in both our previous study<sup>32</sup> and the study of Ziolkowski et al.,<sup>22</sup> and the BPCA-C yields of both compounds in the former study were 74–78% of those in the latter. The time, temperature, and reaction vessels used for nitric acid oxidation in the present study were the same as in our previous work, so a conversion factor of 5.7 was also used here to calculate PAC. An uncertainty of 25% was estimated for the PAC results, as used by Ziolkowski et al.,<sup>22</sup> as the difference in conversion factor was regarded to be systematic between the two studies.

**Selectivity of the BPCA Method to PAC.** The selectivity of the BPCA method for PAC was a matter of concern in the development of this method for the analysis of BC in soils.<sup>21</sup> Humified materials made from ground apple, wet barley straw, and mixtures of arginine and fructose were tested with the BPCA method, and no BPCAs were formed.<sup>21</sup> Thereafter, some other materials were tested, including *Aspergillus niger*,<sup>43</sup> some cyclic carbon forms (chlorophyllin, ellagic acid,  $\beta$ -carotene),<sup>44</sup> oak and grass biomass,<sup>45</sup> and lignin.<sup>46</sup> BPCAs yielded from these materials were not detectable or were detected at very low levels ( $<10$  mg BPCA-C/g OC, Table S3) compared to those from PACs ( $175 \pm 21$  mg BPCA-C/g OC). Moreover, it is not clear whether these low yields of BPCAs were indeed derived from PAC present in these materials as impurities. However, this is likely as shown in our study.

Recently, some nitrophenols, furan derivatives, and methoxyphenols were shown to be key BrC chromophores of biomass burning aerosols by high-resolution MS.<sup>47,48</sup> These chemicals, which are non-PAC but with 1–4 rings in their molecular structures, are suspected to produce BPCAs on treatment with the BPCA method. In the present study, 13 of these BrC chromophores and two analogs (Table S3 and Figure S1) for which standards are commercially available were tested with the BPCA method. The purities of these standards ranged from 95 to 99% (Table S3). It has been reported that some non-PAC materials formed BPCAs only when they were treated in large amounts ( $>5$  mg OC).<sup>44</sup> Therefore, two different weights below and above 5 mg OC were tested.

BPCAs yielded from the standards of BrC chromophores were also not detectable or were present at very low levels ( $\leq 2.05$  mg BPCA-C/g OC, Table S3). In contrast to previous reports,<sup>43,44</sup> the differences in BPCA yields of individual standards in the weights above and below 5 mg OC were not significant. The standard of guaiacol (purity: 98%) showed the highest yield of BPCAs (1.52–2.05 mg BPCA-C/g OC). One more standard of guaiacol with higher purity (99%) purchased from a different supplier was tested but showed lower BPCA yields (0.74–0.81 mg BPCA-C/g OC). This suggests that the BPCAs may be present in the standards as impurities, or may be produced by PAC present in the standards as impurities. That is, the previous and present tests of non-PAC materials with the BPCA method suggested that BPCAs are quite specific molecular markers of PAC.

**Data of Other Carbonaceous Components and Light Absorption.** Analytical methods and data of other components, including organic and elemental carbon of bulk aerosols (OC and EC), water- and methanol-soluble organic carbon (WSOC and MSOC, respectively), and priority PAHs, as well as the UV–visible absorption spectra of WS-BrC and MS-BrC, have been described previously.<sup>12,35,49</sup> These data will be described briefly below.

**OC and BC.** A punch of the filter samples was cut and analyzed for OC and BC using a Desert Research Institute (DRI) Model 2001 thermal/optical reflectance (TOR) carbon analyzer (Atmoslytic Inc., Calabasas, CA) with the Interagency Monitoring of Protected Visual Environment (IMPROVE) protocol.

**WSOC, MSOC, and Priority PAHs.** Filter samples were successively extracted ultrasonically with water and methanol. The water and methanol extracts were filtered with PTFE membranes (0.22  $\mu\text{m}$  pore size). The carbon in the water extracts was measured with a total organic carbon analyzer (Vario TOC tube; Elementar, Hesse, Germany) and used to calculate WSOC.

MSOC was analyzed as described in Lewandowski et al.,<sup>50</sup> Chen et al.,<sup>51</sup> and Tang et al.<sup>12</sup> Briefly, methanol extracts were evaporated to dryness under a gentle stream of high-purity nitrogen gas (99.999%) and redissolved in 500  $\mu\text{L}$  of methanol. A portion of the methanol solution (50  $\mu\text{L}$ ) was slowly spiked onto a 1.5  $\text{cm}^2$  prebaked quartz filter, which was later placed in a desiccator for 24 h to evaporate methanol. Finally, the carbon on the quartz filter was quantified with a DRI TOR carbon analyzer and used to calculate MSOC. As will be described in the Data Quality section, the procedural blanks of MSOC were insignificant and the reproducibility of MSOC quantification was good, which suggested that the methanol loaded onto the filter was completely evaporated and did not lead to a significant overestimate of MSOC.

The methanol extracts were purified with a glass column packed with silica gel and alumina, and then concentrated for the analysis of priority PAHs with GC-MS. Sixteen priority PAHs were measured: naphthalene, acenaphthylene, acenaphthene, fluorene, anthracene, phenanthrene, fluoranthene, pyrene, chrysene, benz[*a*]anthracene, benzo[*b*]fluoranthene, benzo[*k*]fluoranthene, benzo[*a*]pyrene, indeno[1,2,3-*cd*]pyrene, benzo[*g,h,i*]perylene, and dibenz[*a,h*]anthracene.

**UV-Visible Absorption Spectra.** The filter samples were successively extracted ultrasonically with water and methanol. The water and methanol extracts were filtered with PTFE membranes (0.22  $\mu\text{m}$  pore size) and analyzed for UV-visible absorption spectra of WS-BrC and MS-BrC. The UV-visible absorption spectra were recorded in the wavelength range from 200 to 800 nm with intervals of 2 nm. The light absorptivity and wavelength dependence of WS-BrC and MS-BrC are described by the mass absorption efficiency (MAE) and absorption Ångström exponent (AAE).

MAE ( $\text{m}^2 \text{g}^{-1} \text{C}$ ) was calculated as

$$\text{MAE}_\lambda = \frac{A_\lambda}{c \cdot L} \cdot \log(10) \quad (1)$$

where  $A_\lambda$  is the absorbance at a given wavelength  $\lambda$  (nm),  $c$  is the carbon content of WSOC or MSOC ( $\text{mg L}^{-1}$ ), and  $L$  is the absorbing path length (0.01 m). MAEs of WSOC ( $\text{MAE}_{\text{WSOC}}$ ) were calculated for the wavelength range from 250 nm (cutoff wavelength of nitrate) to 580 nm. MAEs of MSOC ( $\text{MAE}_{\text{MSOC}}$ ) were calculated for the wavelength range from 210 nm (cutoff wavelength of methanol) to 700 nm.  $\text{MAE}_{\text{WSOC}}$  and  $\text{MAE}_{\text{MSOC}}$  at longer wavelengths were not investigated due to their low values.

AAE was obtained by

$$A_\lambda = K\lambda^{-\text{AAE}} \quad (2)$$

where  $A_\lambda$  is the absorbance at a given wavelength  $\lambda$  (nm) and  $K$  is a constant. The AAEs of WS-BrC and MS-BrC ( $\text{AAE}_{\text{WS-BrC}}$  and  $\text{AAE}_{\text{MS-BrC}}$ , respectively) were also calculated for wavelengths of 250–580 and 210–700 nm, respectively.

**Data Quality.** At least three blanks and three duplicates were included in each type of measurement. Blanks of WPAC, MPAC, and other carbonaceous components accounted for <5% of their amounts in the samples. The coefficient of variation was <15% for duplicates of WSOC measurements. The coefficients of variation were <8 and <3% for duplicate results of WPAC (or MPAC) and other carbonaceous components, respectively. The absorbances of the field blanks were <0.1% of those of the samples. The coefficient of variation was <1% for duplicates of light absorbance measurements.

## RESULTS AND DISCUSSION

**Occurrence of PAC.** PAC was an important fraction of WSOC and MSOC of OBBA (Figure 3 and Table S1). The contributions of WPAC to WSOC ranged from 2.5 to 18.3% (mean:  $10.3 \pm 3.5\%$ ). The contributions of MPAC to MSOC were even higher (range: 16.1–80.1%, mean:  $45.9 \pm 16.1\%$ ). MPAC was always higher than WPAC for all types of OBBA. The sum of WPAC and MPAC was mostly higher than that of the well-known light absorber BC, suggesting the importance of solvent-extractable PAC as a light absorber. The total amount of the 16 priority PAHs extracted by methanol was <1% of the amount of MPAC. These PAHs are commonly

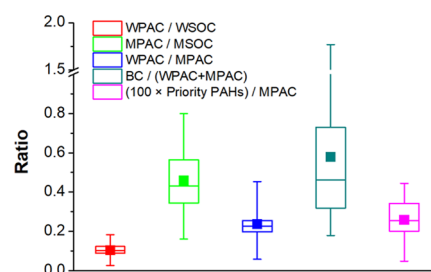


**Figure 3.** Ratios between WPAC (or MPAC) and other carbonaceous components of OBBA.

regarded as priority pollutants and are included in routine measurements. They have been reported to occur in ambient aerosols at similar or higher levels compared with other PAHs and derivatives (e.g., alkylated PAHs, oxygenated PAHs, nitrated PAHs, and chlorinated PAHs), which can be quantified based on available standards.<sup>15–19</sup> Therefore, these PAHs and frequently studied derivatives represent just a small fraction of soluble PAC.

The degree of aromatic condensation was markedly different between WPAC and MPAC, as revealed by the BPCA compositions. Enrichment of BPCAs with more substituted carboxylic groups generally indicates PAC with a higher degree of aromatic condensation.<sup>52,53</sup> The BPCA compositions of WPAC had higher abundance of B3CAs and B2CAs, whereas the BPCA compositions of MPAC had higher abundance of B6CA and B5CA (Figure 4). B4CAs were the predominant BPCAs for both WPAC and MPAC, and their contributions to total BPCAs were also comparable for MPAC and WPAC (mean:  $42.7 \pm 5.4$  vs  $40.7 \pm 3.1\%$ , respectively). We calculated the average number of carboxylic groups for BPCAs ( $N_{\text{COOH}}$ ) of WPAC (or MPAC) by dividing the total amount of BPCAs into the total amount of carboxylic groups of BPCAs (mol/mol). The errors of  $N_{\text{COOH}}$ , which were determined using triplicate samples, were 0.07 and 0.08 for WPAC and MPAC, respectively. The  $N_{\text{COOH}}$  of MPAC ranged from 3.9 to 4.7 (mean:  $4.2 \pm 0.2$ , Figure 4 and Table S4). They were obviously higher than the  $N_{\text{COOH}}$  of WPAC (range: 3.2–3.9, mean  $3.7 \pm 0.2$ ). Therefore, MPAC was more condensed than WPAC.

Both WPAC and MPAC were significantly correlated with other carbonaceous components (priority PAHs, WSOC, MSOC, and OC;  $r \geq 0.62$ ,  $p < 0.01$ , Table S5), except for BC. The correlations between WPAC and MPAC were also strong ( $r = 0.71$ ,  $p < 0.01$ ). BC is regarded as an insoluble highly condensed PAC. The lack of significant correlations between WPAC (or MPAC) and BC may have been due to differences in the burning conditions under which they were formed. That is, a high-temperature combustion favors the formation of components with highly condensed aromatic structures, such as BC, while a low-temperature combustion favors the formation of less condensed aromatic structures, such as MPAC and WPAC.<sup>54</sup>

There was consistency of abundance and molecular structure between MPAC and the priority PAHs. The priority PAH carbon is a fraction of MPAC. The correlation between the abundance of priority PAHs and MPAC was strong ( $r = 0.89$ ,  $p < 0.01$ ). As mentioned above, we used  $N_{\text{COOH}}$  as an indicator of the degree of aromatic condensation of PAC, where a higher  $N_{\text{COOH}}$  indicates more condensed aromatic structures. For the priority PAHs, we also used the ratio between the levels of

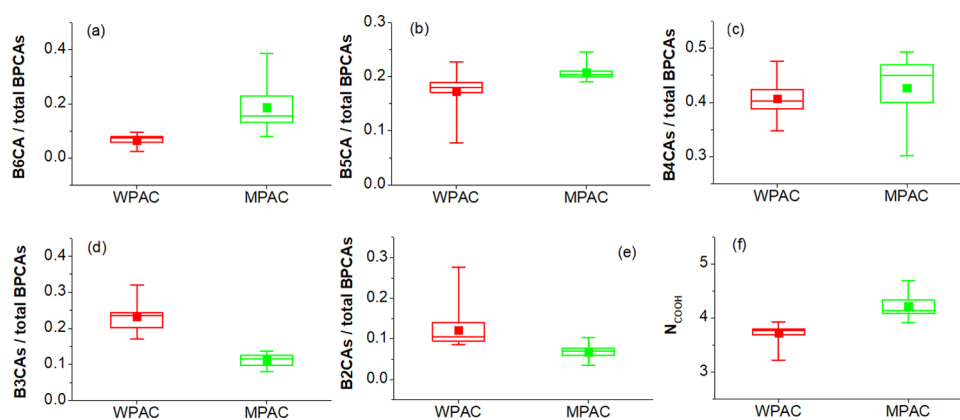


**Figure 4.** BPCA compositions and BPCA average number of carboxylic groups ( $N_{\text{COOH}}$ ) for WPAC and MPAC of OBBA. BPCAs were calculated as carbon contents.

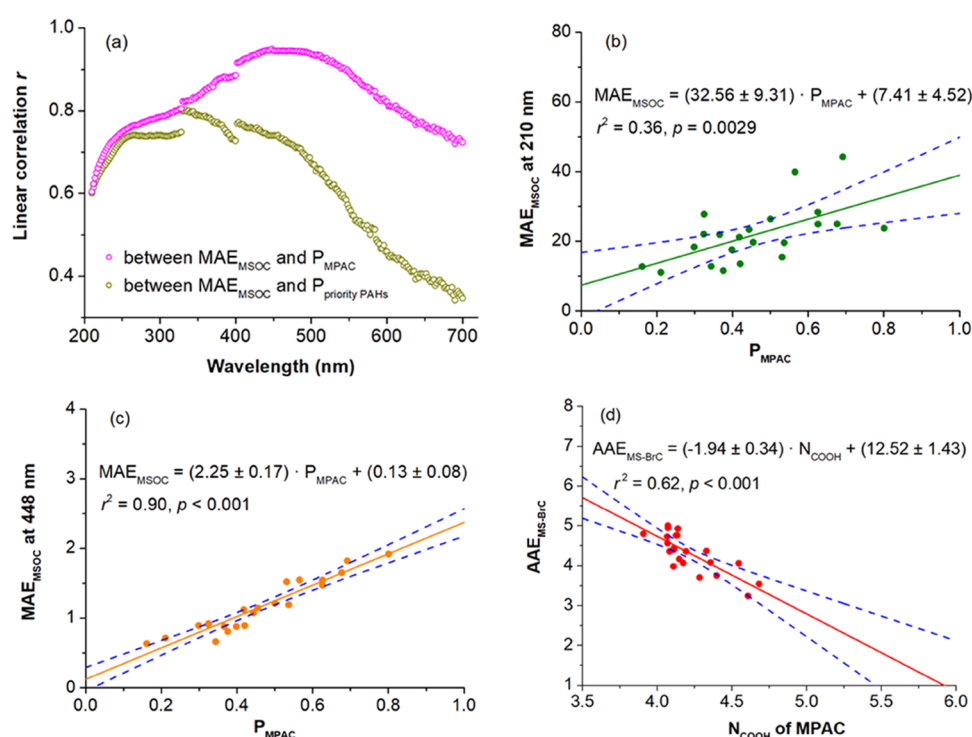


**Figure 5.** Relationships between MPAC and the light absorption properties of MS-BrC. (a)  $r$  values of linear correlations between  $P_{\text{MPAC}}$  (or  $P_{\text{priority PAHs}}$ ) and  $\text{MAE}_{\text{MSOC}}$  at all wavelengths. (b, c) Linear regressions between  $P_{\text{MPAC}}$  and  $\text{MAE}_{\text{MSOC}}$  at representative wavelengths with the lowest and largest  $r^2$  values, respectively. (d) Linear regressions between  $\text{AAE}_{\text{MS-BrC}}$  and  $N_{\text{COOH}}$  of MPAC. Blue dashes in panels (b–d) show 95% confidence bands.

PAHs with 5–6 and 2–4 rings ( $R_{5-6/2-4}$ ) as an indicator of the degree of aromatic condensation, where a larger  $R_{5-6/2-4}$  indicates more condensed molecules.  $R_{5-6/2-4}$  was strongly related to the  $N_{\text{COOH}}$  of MPAC ( $r = 0.76$ ,  $p < 0.01$ ), suggesting consistency of molecular structures between priority PAHs and MPAC. Therefore, the priority PAHs were useful tracers for MPAC of OBBA, although they contributed only a tiny fraction to MPAC. Unlike MPAC, the correlation between the abundance of priority PAHs and WPAC was weaker ( $r = 0.62$ ,  $p < 0.01$ ), and the correlation between  $R_{5-6/2-4}$  and  $N_{\text{COOH}}$  of WPAC was not statistically significant.

**Significance of PAC in Brown Carbon.** PAC is a key fraction determining the light absorption properties of MS-BrC in OBBA, including light absorptivity and wavelength dependence, which were described by the MAEs and AAEs,

respectively. A larger  $\text{MAE}_{\text{MSOC}}$  indicates increased light absorptivity of MS-BrC.  $\text{MAE}_{\text{MSOC}}$  showed a positive linear correlation with the proportion of MPAC in MSOC ( $P_{\text{MPAC}}$ ) at all wavelengths ( $r = 0.60$ – $0.95$ ,  $p < 0.01$ , Figure 5), as did the light absorptivity of MS-BrC. The  $r$  values of the correlation between  $\text{MAE}_{\text{MSOC}}$  and  $P_{\text{MPAC}}$  peaked at 400–500 nm (Figure 5a), suggesting an especially significant influence of MPAC on the light absorptivity of MS-BrC at medium wavelengths. A larger AAE indicates stronger wavelength dependence of MS-BrC.  $\text{AAE}_{\text{MS-BrC}}$  showed a negative linear relation to the  $N_{\text{COOH}}$  of MPAC ( $r = -0.79$ ,  $p < 0.01$ ), suggesting that the wavelength dependence of the light absorption by MS-BrC weakened with increasing aromatic condensation of MPAC. This trend can be explained by physical principles relating light absorption properties to the

molecular structure of carbon. In oscillator theory, electrons are treated as linear oscillators that interact with radiation. Increasing density of  $\pi$ -electrons results in decreases in damping constant and wavelength dependence of light absorption.<sup>55</sup> In band gap theory, increasing cluster size of  $sp^2$ -bonded rings results in decreasing optical gap such that photons of lower energy or longer wavelength can be absorbed.<sup>55,56</sup> In the case where AAE is assumed to be 1, the  $N_{\text{COOH}}$  was  $>5.4$  (95% confidence interval, Figure Sd). This high  $N_{\text{COOH}}$  value indicates BC, which is a highly condensed PAC and mostly generates B6CA in the BPCA method. This result was consistent with the fact that the light absorption of BC is independent of wavelength ( $\text{AAE} \approx 1$ ).<sup>3</sup>

Compared to MPAC, the relation between priority PAHs and the light absorption properties of MS-BrC was weaker, despite the consistency of abundance and molecular structure between MPAC and the priority PAHs. The linear correlation coefficients between the proportion of priority PAHs in MSOC ( $P_{\text{priority PAHs}}$ ) and  $\text{MAE}_{\text{MSOC}}$  peaked in the near-UV range (266–400 nm), and decreased toward shorter or longer wavelengths (Figure Sa). The linear correlation coefficients between  $P_{\text{priority PAHs}}$  and  $\text{MAE}_{\text{MSOC}}$  showed a similar unimodal distribution to those between  $P_{\text{MPAC}}$  and  $\text{MAE}_{\text{MSOC}}$ , but the latter was always higher especially for visible wavelengths (450–700 nm, Figure Sa). This may have been because priority PAHs do not absorb in the visible wavelengths, as reported previously.<sup>34</sup> As mentioned in the previous section, the ratio between levels of 5–6-ring PAHs and 2–4-ring PAHs ( $R_{5-6/2-4}$ ) was used as an indicator of the degree of aromatic condensation, and was strongly related to the  $N_{\text{COOH}}$  of MPAC. However, the correlation between  $R_{5-6/2-4}$  and  $\text{AAE}_{\text{MS-BrC}}$  ( $r = -0.58$ ,  $p = 0.005$ ) was markedly weaker than that between  $N_{\text{COOH}}$  of MPAC and  $\text{AAE}_{\text{MS-BrC}}$  ( $r = -0.79$ ,  $p < 0.001$ ).

It has yet to be determined whether the relation between MPAC and the light absorption properties of MS-BrC observed for the OBBA of rainforest plants in this study are equally valid for other types of biomass burning aerosols. The light absorption properties of bulk biomass burning aerosols depend strongly on the combustion conditions. The effective absorptivity of bulk biomass burning aerosols at a wavelength of 550 nm ( $k_{550}$ ) and its wavelength dependence have been reported to be strongly related to the BC/OA ratio, which is an indicator of combustion efficiency.<sup>57,58</sup> The mass of organic aerosol (i.e., OA) in our study was estimated by multiplying OC by a factor of 2, as in a previous study.<sup>58</sup> The linear correlation coefficient between  $\text{MAE}_{\text{MSOC}}$  and BC/OA increased with wavelength in the range of 210–370 nm ( $r = 0.20$ – $0.40$ ,  $p > 0.050$ ) and was  $0.40$ – $0.48$  ( $p \leq 0.050$ ) at wavelengths of 370–700 nm (Figure S2). Therefore, the correlation between  $\text{MAE}_{\text{MSOC}}$  and BC/OA was weak or not significant. The linear correlation between  $\text{AAE}_{\text{MS-BrC}}$  and BC/OA was also not significant ( $r = -0.35$ ,  $p = 0.11$ ).

However, we still could not conclude that the light absorption properties of MS-BrC were independent of combustion efficiency because some cases of relatively high or low combustion efficiency may have been lacking in our study. We could estimate the combustion conditions of open biomass burning in the present study based on the BC/OC values, as a previous study on open biomass burning reported a relation between BC/OC and modified combustion efficiency (MCE).<sup>59</sup> The MCE involves monitoring of  $\text{CO}_2$  and CO (mainly from smoldering) during a fire. Pure flaming has an

MCE close to 1, while the MCE of smoldering is frequently near 0.8; an MCE near 0.9 suggests roughly equal amounts of biomass consumption by flaming and smoldering.<sup>60</sup> The BC/OC values in our study (0.054–0.57) generally correspond to MCE values between 0.85 and 0.95,<sup>59</sup> suggesting moderate combustion. These combustions did not cover biomass burning dominated more by smoldering (e.g., peatland wildfires) or flaming (e.g., boreal forest fires).

Unlike MS-BrC, a significant relation between PAC and the light absorption properties was not observed for WS-BrC. The light absorptivity and wavelength dependence of the light absorption of OBBA WS-BrC were described by  $\text{MAE}_{\text{WSOC}}$  and  $\text{AAE}_{\text{WS-BrC}}$ . The correlations between  $\text{MAE}_{\text{WSOC}}$  (or  $\text{AAE}_{\text{WS-BrC}}$ ) and the proportion of WPAC in WSOC were not statistically significant, indicating the significance of other chromophores in WS-BrC, such as nitrophenols and polyphenols.<sup>3,6,7</sup>

**Implications and Future Work.** BrC is now recognized as an important component of carbonaceous aerosols that absorbs sunlight and affects radiative forcing. To gain a full understanding of the radiative forcing of BrC, it is essential to clarify its composition and the relationship to the light absorption properties of BrC. However, this is a very challenging task. PAC constitutes a fraction of BrC. Using a novel method, we were able to quantitatively understand the occurrence of WPAC and MPAC in OBBA for the first time. The widely studied priority PAHs contributed  $<1\%$  of MPAC, suggesting that the majority of PAC constituents remain unidentified. WPAC and MPAC are actually analogs of another important light absorber in carbonaceous aerosol, i.e., BC. The sum of WPAC and MPAC was found to be mostly higher than BC for OBBA, suggesting the significance of PAC as a fraction of BrC.

The light absorption properties of PAC could not be investigated directly in this study, but strong linear relations between the abundance of MPAC and light absorptivity of MS-BrC and between the degree of aromatic condensation and wavelength dependence of the light absorption of MS-BrC were observed. These observations suggest that PAC is an important fraction determining the light absorption properties of MS-BrC. Recent studies found strong correlations between PAHs and light absorptivity of MS-BrC in remote and urban regions (Tibetan Plateau and urban Xi'an, China).<sup>34,61</sup> The priority PAHs are useful tracers of MPAC, as found in the present study. Further studies are required to determine whether there are strong relations between MPAC and the light absorptivity of MS-BrC for ambient aerosols. The strong linear relations are probably useful for the prediction of light absorptivities of MS-BrC. The linear relations between  $\text{MAE}_{\text{MSOC}}$  and  $P_{\text{MPAC}}$  observed for OBBA in the present study, mean that the  $\text{MAE}_{\text{MSOC}}$  of OBBA can be estimated by linear regression between  $\text{MAE}_{\text{MSOC}}$  and  $P_{\text{MPAC}}$  (Figure S5b,c) once MPAC and MSOC are quantified. This suggests that the light absorptivity of bulk MS-BrC of OBBA can be estimated despite the complexity of the composition of MS-BrC.

This study showed that the  $N_{\text{COOH}}$  (an indicator of aromatic condensation) differed markedly between different PAC fractions. The  $N_{\text{COOH}}$  of WPAC ( $3.7 \pm 0.2$ ) was different from that of MPAC ( $4.2 \pm 0.2$ ), and both were also different from that of hexane soot ( $N_{\text{COOH}} = 5.5 \pm 0.2$ ),<sup>53</sup> which can be used as a reference material for aerosol BC. PAC in the remaining particles after water and methanol extraction (RPAC) was also analyzed with the BPCA method in this

study, but the data are not reported here considering the poor reproducibility due to significant particle loss during the extraction procedures. RPAC may contain BC and other insoluble PAC. The latter is a seldom studied BrC fraction.<sup>62</sup> The markedly lower  $N_{\text{COOH}}$  of RPAC in the present study ( $4.5 \pm 0.3$ ) compared to that of BC indicated, at least, the existence of insoluble non-BC PAC (i.e., insoluble BrC). The extraction methods used in the present study should be optimized in future to accurately quantify RPAC, to allow the investigation of insoluble BrC.

Atmospheric aging of BrC can also be studied by a combination of BrC fractionation and PAC characterization with the BPCA method. The atmospheric aging of BrC is another challenging task in studies of the light absorption properties of BrC. PAC in atmospheric aerosols is generated by combustion of organic matter and not produced in atmospheric aging processes. PAC can be oxidized during atmospheric transport. The oxidation of PAC may lead to an increase in polarity and a decrease in aromatic condensation. An increase in polarity can be investigated by quantifying the abundance of PAC in BrC fractionated by solvents of different polarities. A decrease in aromatic condensation can be indicated by changes in  $N_{\text{COOH}}$ . Further studies are required to study the oxidation of PAC during atmospheric transport and its impact on the light absorption properties of BrC.

## ■ ASSOCIATED CONTENT

### Supporting Information

The Supporting Information is available free of charge at <https://pubs.acs.org/doi/10.1021/acs.est.1c06460>.

Details of collection of open biomass burning aerosols (Section S1); ratios between WPAC (or MPAC) and other carbonaceous components of OBBA (Table S1); mixing gradient of mobile phases for the HPLC method of BPCA analysis (Table S2); compilation of BPCA carbon yielded from non-PAC materials (Table S3); BPCA compositions and BPCAs' average number of carboxylic groups ( $N_{\text{COOH}}$ ) for WPAC and MPAC of OBBA (Table S4);  $r$  values of Pearson's correlation between WPAC (or MPAC) and other carbonaceous components (Table S5); molecular structures of BrC chromophores, which were tested with the BPCA method in our study (Figure S1); and  $r$  value of linear correlation between  $\text{MAE}_{\text{MSOC}}$  and BC/OA (Figure S2) (PDF)

## ■ AUTHOR INFORMATION

### Corresponding Authors

**Guangcai Zhong** – State Key Laboratory of Organic Geochemistry and Guangdong-Hongkong-Macao Joint Laboratory for Environmental Pollution and Control, Guangzhou Institute of Geochemistry, Chinese Academy of Sciences, Guangzhou 510640, P. R. China; [orcid.org/0000-0002-5647-5940](https://orcid.org/0000-0002-5647-5940); Phone: +86-20-38350480; Email: [gczhong@gig.ac.cn](mailto:gczhong@gig.ac.cn)

**Gan Zhang** – State Key Laboratory of Organic Geochemistry and Guangdong-Hongkong-Macao Joint Laboratory for Environmental Pollution and Control, Guangzhou Institute of Geochemistry, Chinese Academy of Sciences, Guangzhou 510640, P. R. China; [orcid.org/0000-0002-9010-8140](https://orcid.org/0000-0002-9010-8140); Phone: +86-20-85290805; Email: [zhanggan@gig.ac.cn](mailto:zhanggan@gig.ac.cn)

## Authors

**Yue Sun** – State Key Laboratory of Organic Geochemistry and Guangdong-Hongkong-Macao Joint Laboratory for Environmental Pollution and Control, Guangzhou Institute of Geochemistry, Chinese Academy of Sciences, Guangzhou 510640, P. R. China; University of Chinese Academy of Sciences, Beijing 100049, P. R. China

**Jiao Tang** – State Key Laboratory of Organic Geochemistry and Guangdong-Hongkong-Macao Joint Laboratory for Environmental Pollution and Control, Guangzhou Institute of Geochemistry, Chinese Academy of Sciences, Guangzhou 510640, P. R. China; [orcid.org/0000-0001-5485-8174](https://orcid.org/0000-0001-5485-8174)

**Yangzhi Mo** – State Key Laboratory of Organic Geochemistry and Guangdong-Hongkong-Macao Joint Laboratory for Environmental Pollution and Control, Guangzhou Institute of Geochemistry, Chinese Academy of Sciences, Guangzhou 510640, P. R. China; [orcid.org/0000-0002-6075-3421](https://orcid.org/0000-0002-6075-3421)

**Xiaofei Geng** – State Key Laboratory of Organic Geochemistry and Guangdong-Hongkong-Macao Joint Laboratory for Environmental Pollution and Control, Guangzhou Institute of Geochemistry, Chinese Academy of Sciences, Guangzhou 510640, P. R. China; Nanjing Institute of Environmental Sciences, Ministry of Ecology and Environment of the People's Republic of China, 210042 Nanjing, China

**Xin Yi** – State Key Laboratory of Organic Geochemistry and Guangdong-Hongkong-Macao Joint Laboratory for Environmental Pollution and Control, Guangzhou Institute of Geochemistry, Chinese Academy of Sciences, Guangzhou 510640, P. R. China; University of Chinese Academy of Sciences, Beijing 100049, P. R. China

**Caiqing Yan** – Environment Research Institute, Shandong University, Qingdao 266000, P. R. China

**Jun Li** – State Key Laboratory of Organic Geochemistry and Guangdong-Hongkong-Macao Joint Laboratory for Environmental Pollution and Control, Guangzhou Institute of Geochemistry, Chinese Academy of Sciences, Guangzhou 510640, P. R. China; [orcid.org/0000-0002-3637-1642](https://orcid.org/0000-0002-3637-1642)

Complete contact information is available at: <https://pubs.acs.org/doi/10.1021/acs.est.1c06460>

## Author Contributions

Y.S. did the PAC analysis, analyzed the data, and wrote the manuscript; J.T. carried out aerosol sampling, analysis of WSOC and MSOC, and light absorption of WSOC and MSOC; J.T., Y.M., C.Y., and J.L. provided valuable suggestions and discussions on the writing of this manuscript; X.G. and X.Y. assisted with the PAC analysis using the BPCA method; G.Z. guided through the technical experiments, data analysis, and manuscript organization; G.Z. inspired and designed the study.

## Notes

The authors declare no competing financial interest.

## ■ ACKNOWLEDGMENTS

This work is supported by the National Natural Science Foundation of China (No. 42030715), the State Key Laboratory of Organic Geochemistry, GIGCAS (No. SKLOG2020-3), and the Guangdong Foundation for Program of Science and Technology Research (No. 2019B121205006). The authors appreciate Yankuan Tian for the maintenance of GC-MS and Jiazhao He for the maintenance of the TOC

carbon analyzer. We appreciate the comments and suggestions given by all anonymous reviewers of this study.

## REFERENCES

- (1) Andreae, M. O.; Gelencser, A. Black carbon or brown carbon? The nature of light-absorbing carbonaceous aerosols. *Atmos. Chem. Phys.* **2006**, *6*, 3131–3148.
- (2) Chung, S. H.; Seinfeld, J. H. Global distribution and climate forcing of carbonaceous aerosols. *J. Geophys. Res.: Atmos.* **2002**, *107*, No. 4407.
- (3) Laskin, A.; Laskin, J.; Nizkorodov, S. A. Chemistry of Atmospheric Brown Carbon. *Chem. Rev.* **2015**, *115*, 4335–4382.
- (4) Bond, T. C.; Doherty, S. J.; Fahey, D. W.; Forster, P. M.; Berntsen, T.; DeAngelo, B. J.; Flanner, M. G.; Ghan, S.; Karcher, B.; Koch, D.; Kinne, S.; Kondo, Y.; Quinn, P. K.; Sarofim, M. C.; Schultz, M. G.; Schulz, M.; Venkataraman, C.; Zhang, H.; Zhang, S.; Bellouin, N.; Guttikunda, S. K.; Hopke, P. K.; Jacobson, M. Z.; Kaiser, J. W.; Klimont, Z.; Lohmann, U.; Schwarz, J. P.; Shindell, D.; Storelvmo, T.; Warren, S. G.; Zender, C. S. Bounding the role of black carbon in the climate system: A scientific assessment. *J. Geophys. Res.: Atmos.* **2013**, *118*, 5380–5552.
- (5) Chen, Y.; Bond, T. C. Light absorption by organic carbon from wood combustion. *Atmos. Chem. Phys.* **2010**, *10*, 1773–1787.
- (6) Lin, P.; Aiona, P. K.; Li, Y.; Shiraiwa, M.; Laskin, J.; Nizkorodov, S. A.; Laskin, A. Molecular Characterization of Brown Carbon in Biomass Burning Aerosol Particles. *Environ. Sci. Technol.* **2016**, *50*, 11815–11824.
- (7) Lin, P.; Fleming, L. T.; Nizkorodov, S. A.; Laskin, J.; Laskin, A. Comprehensive Molecular Characterization of Atmospheric Brown Carbon by High Resolution Mass Spectrometry with Electrospray and Atmospheric Pressure Photoionization. *Anal. Chem.* **2018**, *90*, 12493–12502.
- (8) Mahamuni, G.; Rutherford, J.; Davis, J.; Molnar, E.; Posner, J. D.; Seto, E.; Korshin, G.; Novosselov, I. Excitation-Emission Matrix Spectroscopy for Analysis of Chemical Composition of Combustion Generated Particulate Matter. *Environ. Sci. Technol.* **2020**, *54*, 8198–8209.
- (9) Chen, Q. C.; Ikemori, F.; Mochida, M. Light Absorption and Excitation-Emission Fluorescence of Urban Organic Aerosol Components and Their Relationship to Chemical Structure. *Environ. Sci. Technol.* **2016**, *50*, 10859–10868.
- (10) Li, M. J.; Fan, X. J.; Zhu, M. B.; Zou, C. L.; Song, J. Z.; Wei, S. Y.; Jia, W. L.; Peng, P. A. Abundance and Light Absorption Properties of Brown Carbon Emitted from Residential Coal Combustion in China. *Environ. Sci. Technol.* **2019**, *53*, 595–603.
- (11) Tóth, A.; Hoffer, A.; Posfai, M.; Ajtai, T.; Konya, Z.; Blazso, M.; Czegeny, Z.; Kiss, G.; Bozoki, Z.; Gelencser, A. Chemical characterization of laboratory-generated tar ball particles. *Atmos. Chem. Phys.* **2018**, *18*, 10407–10418.
- (12) Tang, J.; Li, J.; Su, T.; Han, Y.; Mo, Y. Z.; Jiang, H. X.; Cui, M.; Jiang, B.; Chen, Y. J.; Tang, J. H.; Song, J. Z.; Peng, P. A.; Zhang, G. Molecular compositions and optical properties of dissolved brown carbon in biomass burning, coal combustion, and vehicle emission aerosols illuminated by excitation-emission matrix spectroscopy and Fourier transform ion cyclotron resonance mass spectrometry analysis. *Atmos. Chem. Phys.* **2020**, *20*, 2513–2532.
- (13) Huang, R. J.; Yang, L.; Shen, J. C.; Yuan, W.; Gong, Y. Q.; Guo, J.; Cao, W. J.; Duan, J.; Ni, H. Y.; Zhu, C. S.; Dai, W. T.; Li, Y. J.; Chen, Y.; Chen, Q.; Wu, Y. F.; Zhang, R. J.; Dusek, U.; O'Dowd, C.; Hoffmann, T. Water-Insoluble Organics Dominate Brown Carbon in Wintertime Urban Aerosol of China: Chemical Characteristics and Optical Properties. *Environ. Sci. Technol.* **2020**, *54*, 7836–7847.
- (14) Lima, A. L. C.; Farrington, J. W.; Reddy, C. M. Combustion-derived polycyclic aromatic hydrocarbons in the environment - A review. *Environ. Forensics* **2005**, *6*, 109–131.
- (15) Albinet, A.; Leoz-Garziandia, E.; Budzinski, H.; Villenave, E. Polycyclic aromatic hydrocarbons (PAHs), nitrated PAHs and oxygenated PAHs in ambient air of the Marseilles area (South of France): Concentrations and sources. *Sci. Total Environ.* **2007**, *384*, 280–292.
- (16) Bamford, H. A.; Bezabeh, D. Z.; Schantz, M. M.; Wise, S. A.; Baker, J. E. Determination and comparison of nitrated-polycyclic aromatic hydrocarbons measured in air and diesel particulate reference materials. *Chemosphere* **2003**, *50*, 575–587.
- (17) Bandowe, B. A. M.; Meusel, H.; Huang, R. J.; Ho, K. F.; Cao, J. J.; Hoffmann, T.; Wilcke, W. PM<sub>2.5</sub>-bound oxygenated PAHs, nitro-PAHs and parent-PAHs from the atmosphere of a Chinese megacity: Seasonal variation, sources and cancer risk assessment. *Sci. Total Environ.* **2014**, *473–474*, 77–87.
- (18) Jin, R.; Liu, G. R.; Jiang, X. X.; Liang, Y.; Fiedler, H.; Yang, L. L.; Zhu, Q. Q.; Xu, Y.; Gao, L. R.; Su, G. J.; Xiao, K.; Zheng, M. H. Profiles, sources and potential exposures of parent, chlorinated and brominated polycyclic aromatic hydrocarbons in haze associated atmosphere. *Sci. Total Environ.* **2017**, *593–584*, 390–398.
- (19) Nocun, M. S.; Schantz, M. M. Determination of selected oxygenated polycyclic aromatic hydrocarbons (oxy-PAHs) in diesel and air particulate matter standard reference materials (SRMs). *Anal. Bioanal. Chem.* **2013**, *405*, 5583–5593.
- (20) Samburova, V.; Connolly, J.; Gyawali, M.; Yatavelli, R. L. N.; Watts, A. C.; Chakrabarty, R. K.; Zielinska, B.; Moosmuller, H.; Khlystov, A. Polycyclic aromatic hydrocarbons in biomass-burning emissions and their contribution to light absorption and aerosol toxicity. *Sci. Total Environ.* **2016**, *568*, 391–401.
- (21) Glaser, B.; Haumaier, L.; Guggenberger, G.; Zech, W. Black carbon in soils: the use of benzenecarboxylic acids as specific markers. *Org. Geochem.* **1998**, *29*, 811–819.
- (22) Ziolkowski, L. A.; Chamberlin, A. R.; Greaves, J.; Druffel, E. R. M. Quantification of black carbon in marine systems using the benzene polycarboxylic acid method: a mechanistic and yield study. *Limnol. Oceanogr.: Methods* **2011**, *9*, 140–149.
- (23) Dittmar, T. The molecular level determination of black carbon in marine dissolved organic matter. *Org. Geochem.* **2008**, *39*, 396–407.
- (24) Wagner, S.; Brandes, J.; Spencer, R. G. M.; Ma, K.; Rosengard, S. Z.; Moura, J. M. S.; Stubbins, A. Isotopic composition of oceanic dissolved black carbon reveals non-riverine source. *Nat. Commun.* **2019**, *10*, No. 5064.
- (25) Coppola, A. I.; Seidel, M.; Ward, N. D.; Viviroli, D.; Nascimento, G. S.; Haghypour, N.; Revels, B. N.; Abiven, S.; Jones, M. W.; Richey, J. E.; Eglinton, T. I.; Dittmar, T.; Schmidt, M. W. I. Marked isotopic variability within and between the Amazon River and marine dissolved black carbon pools. *Nat. Commun.* **2019**, *10*, No. 4018.
- (26) Khan, A. L.; Wagner, S.; Jaffe, R.; Xian, P.; Williams, M.; Armstrong, R.; McKnight, D. Dissolved black carbon in the global cryosphere: Concentrations and chemical signatures. *Geophys. Res. Lett.* **2017**, *44*, 6226–6234.
- (27) Jaffé, R.; Ding, Y.; Niggemann, J.; Vahatalo, A. V.; Stubbins, A.; Spencer, R. G. M.; Campbell, J.; Dittmar, T. Global Charcoal Mobilization from Soils via Dissolution and Riverine Transport to the Oceans. *Science* **2013**, *340*, 345–347.
- (28) Ding, Y.; Yamashita, Y.; Dodds, W. K.; Jaffe, R. Dissolved black carbon in grassland streams: Is there an effect of recent fire history? *Chemosphere* **2013**, *90*, 2557–2562.
- (29) Coppola, A. I.; Ziolkowski, L. A.; Masiello, C. A.; Druffel, E. R. M. Aged black carbon in marine sediments and sinking particles. *Geophys. Res. Lett.* **2014**, *41*, 2427–2433.
- (30) Coppola, A. I.; Wiedemeier, D. B.; Galy, V.; Haghypour, N.; Hanke, U. M.; Nascimento, G. S.; Usman, M.; Blattmann, T. M.; Reisser, M.; Freymond, C. V.; Zhao, M. X.; Voss, B.; Wacker, L.; Schefuss, E.; Peucker-Ehrenbrink, B.; Abiven, S.; Schmidt, M. W. I.; Eglinton, T. I. Global-scale evidence for the refractory nature of riverine black carbon. *Nat. Geosci.* **2018**, *11*, 584–588.
- (31) Bao, H. Y.; Niggemann, J.; Luo, L.; Dittmar, T.; Kao, S. J. Aerosols as a source of dissolved black carbon to the ocean. *Nat. Commun.* **2017**, *8*, No. 510.

- (32) Zhong, G. C.; Sun, Y.; Geng, X. F.; Yi, X.; Zhang, G. Benzene polycarboxylic acid characterisation of polyaromatics in ambient aerosol: Method development. *Atmos. Environ.* **2019**, *211*, 55–62.
- (33) Bond, T. C.; Streets, D. G.; Yarber, K. F.; Nelson, S. M.; Woo, J. H.; Klimont, Z. A technology-based global inventory of black and organic carbon emissions from combustion. *J. Geophys. Res.: Atmos.* **2004**, *109*, No. D14203.
- (34) Huang, R. J.; Yang, L.; Cao, J. J.; Chen, Y.; Chen, Q.; Li, Y. J.; Duan, J.; Zhu, C. S.; Dai, W. T.; Wang, K.; Lin, C. S.; Ni, H. Y.; Corbin, J. C.; Wu, Y. F.; Zhang, R. J.; Tie, X. X.; Hoffmann, T.; O'Dowd, C.; Dusek, U. Brown Carbon Aerosol in Urban Xi'an, Northwest China: The Composition and Light Absorption Properties. *Environ. Sci. Technol.* **2018**, *52*, 6825–6833.
- (35) Cui, M.; Chen, Y. J.; Zheng, M.; Li, J.; Tang, J.; Han, Y.; Song, D. B.; Yan, C. Q.; Zhang, F.; Tian, C. G.; Zhang, G. Emissions and characteristics of particulate matter from rainforest burning in the Southeast Asia. *Atmos. Environ.* **2018**, *191*, 194–204.
- (36) Tang, J.; Li, J.; Mo, Y. Z.; Khorram, M. S.; Chen, Y. J.; Tang, J. H.; Zhang, Y. L.; Song, J. Z.; Zhang, G. Light absorption and emissions inventory of humic-like substances from simulated rainforest biomass burning in Southeast Asia. *Environ. Pollut.* **2020**, *262*, No. 114266.
- (37) Hindersmann, B.; Achten, C. Accelerated benzene polycarboxylic acid analysis by liquid chromatography-time-of-flight-mass spectrometry for the determination of petrogenic and pyrogenic carbon. *J. Chromatogr. A* **2017**, *1510*, 57–65.
- (38) Wiedemeier, D. B.; Hilf, M. D.; Smittenberg, R. H.; Haberle, S. G.; Schmidt, M. W. I. Improved assessment of pyrogenic carbon quantity and quality in environmental samples by high-performance liquid chromatography. *J. Chromatogr. A* **2013**, *1304*, 246–250.
- (39) Wiedemeier, D. B.; Lang, S. Q.; Gierga, M.; Abiven, S.; Bernasconi, S. M.; Fruh-Green, G. L.; Hajdas, I.; Hanke, U. M.; Hilf, M. D.; McIntyre, C. P.; Scheider, M. P. W.; Smittenberg, R. H.; Wacker, L.; Wiesenberg, G. L. B.; Schmidt, M. W. I. Characterization, Quantification and Compound-specific Isotopic Analysis of Pyrogenic Carbon Using Benzene Polycarboxylic Acids (BPCA). *JOVE-J. Vis. Exp.* **2016**, *2016*, No. 53922.
- (40) Yassine, M. M.; Suski, M.; Dabek-Zlotorzynska, E. Characterization of benzene polycarboxylic acids and polar nitroaromatic compounds in atmospheric aerosols using UPLC-MS/MS. *J. Chromatogr. A* **2020**, *1630*, No. 461507.
- (41) Sheesley, R. J.; Deminter, J. T.; Meiritz, M.; Snyder, D. C.; Schauer, J. J. Temporal Trends in Motor Vehicle and Secondary Organic Tracers Using in Situ Methylation Thermal Desorption GCMS. *Environ. Sci. Technol.* **2010**, *44*, 9398–9404.
- (42) He, X.; Huang, X. H. H.; Chow, K. S.; Wang, Q. Q.; Zhang, T.; Wu, D.; Yu, J. Z. Abundance and Sources of Phthalic Acids, Benzene-Tricarboxylic Acids, and Phenolic Acids in PM<sub>2.5</sub> at Urban and Suburban Sites in Southern China. *ACS Earth and Space Chem.* **2018**, *2*, 147–158.
- (43) Brodowski, S.; Rodionov, A.; Haumaier, L.; Glaser, B.; Amelung, W. Revised black carbon assessment using benzene polycarboxylic acids. *Org. Geochem.* **2005**, *36*, 1299–1310.
- (44) Kappenberg, A.; Blasing, M.; Lehndorff, E.; Amelung, W. Black carbon assessment using benzene polycarboxylic acids: Limitations for organic-rich matrices. *Org. Geochem.* **2016**, *94*, 47–51.
- (45) Bostick, K. W.; Zimmerman, A. R.; Wozniak, A. S.; Mitra, S.; Hatcher, P. G. Production and Composition of Pyrogenic Dissolved Organic Matter From a Logical Series of Laboratory-Generated Chars. *Front. Earth Sci.* **2018**, *6*, No. 43.
- (46) Chang, Z.; Tian, L.; Li, F.; Zhou, Y.; Wu, M.; Steinberg, C. E. W.; Dong, X.; Pan, B.; Xing, B. Benzene polycarboxylic acid - A useful marker for condensed organic matter, but not for only pyrogenic black carbon. *Sci. Total Environ.* **2018**, *626*, 660–667.
- (47) Hettiyadura, A. P. S.; Garcia, V.; Li, C. L.; West, C. P.; Tomlin, J.; He, Q. F.; Rudich, Y.; Laskin, A. Chemical Composition and Molecular-Specific Optical Properties of Atmospheric Brown Carbon Associated with Biomass Burning. *Environ. Sci. Technol.* **2021**, *55*, 2511–2521.
- (48) Li, X.; Hu, M.; Wang, Y. J.; Xu, N.; Fan, H. Y.; Zong, T. M.; Wu, Z. J.; Guo, S.; Zhu, W. F.; Chen, S. Y.; Dong, H. B.; Zeng, L. M.; Yu, X. N.; Tang, X. Y. Links between the optical properties and chemical compositions of brown carbon chromophores in different environments: Contributions and formation of functionalized aromatic compounds. *Sci. Total Environ.* **2021**, *786*, No. 147418.
- (49) Mao, S. D.; Zhang, G.; Zhao, S. Z.; Li, J.; Liu, X.; Cheng, Z. N.; Zhong, G. C.; Malik, R. N.; Liu, X. High Abundance of Unintentionally Produced Tetrachlorobiphenyls (PCB47/48/75, 51, and 68) in the Atmosphere at a Regional Background Site in East China. *Environ. Sci. Technol.* **2019**, *53*, 3464–3470.
- (50) Lewandowski, M.; Jaoui, M.; Kleindienst, T. E.; Offenber, J. H.; Edney, E. O. Composition of PM<sub>2.5</sub> during the summer of 2003 in Research Triangle Park, North Carolina. *Atmos. Environ.* **2007**, *41*, 4073–4083.
- (51) Chen, Q.; Ikemori, F.; Nakamura, Y.; Vodicka, P.; Kawamura, K.; Mochida, M. Structural and Light-Absorption Characteristics of Complex Water-Insoluble Organic Mixtures in Urban Submicrometer Aerosols. *Environ. Sci. Technol.* **2017**, *51*, 8293–8303.
- (52) Wiedemeier, D. B.; Abiven, S.; Hockaday, W. C.; Keiluweit, M.; Kleber, M.; Masiello, C. A.; McBeath, A. V.; Nico, P. S.; Pyle, L. A.; Schneider, M. P. W.; Smernik, R. J.; Wiesenberg, G. L. B.; Schmidt, M. W. I. Aromaticity and degree of aromatic condensation of char. *Org. Geochem.* **2015**, *78*, 135–143.
- (53) Ziolkowski, L. A.; Druffel, E. R. M. Aged black carbon identified in marine dissolved organic carbon. *Geophys. Res. Lett.* **2010**, *37*, No. L16601.
- (54) Bird, M. I.; Wynn, J. G.; Saiz, G.; Wurster, C. M.; McBeath, A. The Pyrogenic Carbon Cycle. *Annu. Rev. Earth Planet. Sci.* **2015**, *43*, 273–298.
- (55) Bond, T. C.; Bergstrom, R. W. Light absorption by carbonaceous particles: An investigative review. *Aerosol Sci. Technol.* **2006**, *40*, 27–67.
- (56) Bond, T. C. Spectral dependence of visible light absorption by carbonaceous particles emitted from coal combustion. *Geophys. Res. Lett.* **2001**, *28*, 4075–4078.
- (57) Saleh, R.; Robinson, E. S.; Tkacik, D. S.; Ahern, A. T.; Liu, S.; Aiken, A. C.; Sullivan, R. C.; Presto, A. A.; Dubey, M. K.; Yokelson, R. J.; Donahue, N. M.; Robinson, A. L. Brownness of organics in aerosols from biomass burning linked to their black carbon content. *Nat. Geosci.* **2014**, *7*, 647–650.
- (58) Lu, Z. F.; Streets, D. G.; Winijkul, E.; Yan, F.; Chen, Y. J.; Bond, T. C.; Feng, Y.; Dubey, M. K.; Liu, S.; Pinto, J. P.; Carmichael, G. R. Light Absorption Properties and Radiative Effects of Primary Organic Aerosol Emissions. *Environ. Sci. Technol.* **2015**, *49*, 4868–4877.
- (59) McMeeking, G. R.; Kreidenweis, S. M.; Baker, S.; Carrico, C. M.; Chow, J. C.; Collett, J. L.; Hao, W. M.; Holden, A. S.; Kirchstetter, T. W.; Malm, W. C.; Moosmuller, H.; Sullivan, A. P.; Wold, C. E. Emissions of trace gases and aerosols during the open combustion of biomass in the laboratory. *J. Geophys. Res.: Atmos.* **2009**, *114*, No. D19210.
- (60) Akagi, S. K.; Yokelson, R. J.; Wiedinmyer, C.; Alvarado, M. J.; Reid, J. S.; Karl, T.; Crounse, J. D.; Wennberg, P. O. Emission factors for open and domestic biomass burning for use in atmospheric models. *Atmos. Chem. Phys.* **2011**, *11*, 4039–4072.
- (61) Zhu, C. S.; Li, L. J.; Huang, H.; Dai, W. T.; Lei, Y. L.; Qu, Y.; Huang, R. J.; Wang, Q. Y.; Shen, Z. X.; Cao, J. J. n-Alkanes and PAHs in the Southeastern Tibetan Plateau: Characteristics and Correlations With Brown Carbon Light Absorption. *J. Geophys. Res.: Atmos.* **2020**, *125*, No. e2020JD032666.
- (62) Bai, Z.; Zhang, L. Y.; Cheng, Y.; Zhang, W.; Mao, J. F.; Chen, H.; Li, L.; Wang, L. N.; Chen, J. M. Water/Methanol-Insoluble Brown Carbon Can Dominate Aerosol-Enhanced Light Absorption in Port Cities. *Environ. Sci. Technol.* **2020**, *54*, 14889–14898.